

SCANNING TUNNELING LUMINESCENCE OF MOLECULES AND NANOSTRUCTURES

Laura B. Ruppalt
PHYS598OS Final Paper
December 13, 2005

Abstract:

By coupling a standard scanning tunneling microscope to a photon collection and detection system, scanning tunneling luminescence (STL) microscopy provides a means of optically characterizing conducting and semiconducting specimens with nanometer-scale spatial resolution. The following report provides an overview of the STL technique, including a review of the basic physical mechanisms leading to tunneling-carrier-induced luminescence, as well as a survey of current instrumental approaches to implementing an effective STL system, with particular focus on lens, optical fiber, and conductive transparent tip photon collection schemes. Two recent examples of STL applied to the analysis of organic molecules (Zn(II)-etioporphyrin I) and inorganic nanostructures (III/V-semiconductor based embedded quantum dots) are highlighted. Additionally, a brief proposal for the use of STL towards the optical characterization of single-walled carbon nanotubes is discussed.

Since the first published observation of light emission from a scanning tunneling microscope (STM) by Gimzewski and co-workers at IBM's Zurich Research Laboratory in 1988,¹ scanning tunneling luminescence (STL), as the phenomenon has come to be called, has found a niche among optical characterization techniques for its ability to provide a wide range of optical information from a surface with incomparable spatial resolving capabilities. STL, also commonly referred to as "scanning tunneling microscope light emission spectroscopy" (STM-LES) or simply "tunneling luminescence" (TL) spectroscopy, combines the atomic-level lateral sensitivity of the STM with detailed photon emission spectroscopic measurements to optically characterize structures on a nanometer length scale.

In conventional STM, a metallic tip and conductive or semi-conductive sample are brought into close range, with no actual physical contact made between the two. If the two are near enough to each other, a bias voltage applied between the tip and sample will induce a small but finite "tunneling current" to flow across the gap between the two electrodes. For cases in which the sample potential is positive with respect to the tip potential, electrons will be injected from the tip into the sample. In a like manner, sample potentials which are negative with respect to the tip potential will cause electrons to flow from the sample to the tip and induce a current which can equivalently be thought of as composed of "holes" of mass equal to that of an electron but with a charge of $+q$, opposite in sign but equal in magnitude to the single electron charge, flowing in the opposite direction, from tip to sample.

Under certain circumstances, an electron or hole injected into a sample from the tip during the tunneling process can generate the emission of a photon from the tunnel junction gap with a quantum efficiency generally on the order of 10^{-4} photons/injected carrier.² It is these emitted photons which are collected and analyzed in STL measurements and which can provide valuable information regarding the optical properties of the nanostructures under study.

In a typical STL experiment, while the STM tip is rastered across the region of interest and tunneling current information is logged, additional instrumentation also records the intensity and/or wavelength of any light emission induced by the electron tunneling process at a given spatial location. This information can be collected and analyzed in variety of ways to reveal a wealth of information regarding the optical nature of the probed sample. Gimzewski, et. al. identify four primary STL operational modes in their seminal paper, with representative data illustrated in Figure 1:¹

1. Isochromat spectroscopy: A single photon energy is monitored as the tip-sample potential difference, and thus injected tunneling electron energy, is ramped through a specified range-comparable to excitation spectroscopy in standard fluorescence measurements.

2. Fluorescence spectroscopy: The spectral distribution of emitted photons is monitored and recorded while the tunneling electron energy is held steady through the use of a constant applied tip-sample bias- comparable to emission spectroscopy in standard fluorescence measurements.

3. Luminescence spectroscopy: A special case of fluorescence spectroscopy unique to semiconducting samples in which injected electrons relax to the conduction band edge (CBE) before recombining across the semiconducting bandgap. Generally, all injected tunneling electrons with energy greater than the CBE energy give rise to similar photon emission spectra.

4. Spatial mapping: A specified feature observed in spectra acquired in isochromat, fluorescence, or luminescence modes is plotted as a function of lateral tip position, producing a spatial mapping of the given optical characteristic. For example, photon maps of total emitted photon intensity, or wavelength specific photon intensity can be constructed, allowing one to discriminate areas of differing optical character on the sample.

As highlighted earlier, the primary benefit of scanning tunneling luminescence microscopy over other luminescence probe approaches is the high spatial resolution achievable by this technique- the lateral resolution capabilities of the STM allow the correlation of specific light emission characteristics with nano- (potentially even sub nano-) scale features in STL. The spatial resolution of a given STL measurement is determined by three primary factors:

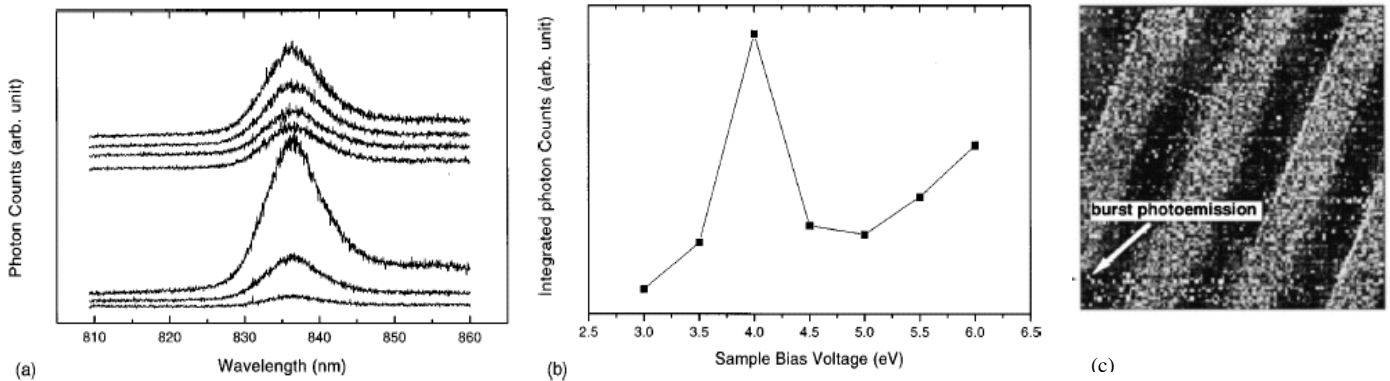


Figure 1: Examples of the various optical information that can be obtained via STL measurements: (a) Fluorescence/luminescence spectra of GaAs substrate showing clear exciton energy emission peak at ~838 nm, near the GaAs bandgap value. Multiple spectra were acquired by varying the sample bias.⁴ (b) The isochromat corresponding to the total photon intensity at the peak values of the spectra plotted in (a).⁴ It can be seen that maximum 838 nm emission intensity is detected when the sample bias is held at ~4.0 V. (c) Spatial photon map of a GaAs/AlAs multiple quantum well structure. Bright regions correspond to the light emitting GaAs wells.³

1. STM tip radius: The shape and size of the STM tip apex determines the extent of the “beam” of tunneling electrons between tip and sample, and, as luminescence originates primarily from the sample region directly illuminated by tunneling electrons, the sharper the tip, the more narrow the electron “beam,” and the more localized the luminescence. Conventional STM-ers consistently achieve atomic resolution imaging, indicating that the extent of the tunneling “beam” can be in the angstrom or sub-angstrom range.

2. Diffusion of injected carriers: The full spatial extent of the luminescent region will be determined by the length scale over which injected carriers can diffuse and recombine to produce light. This length scale is primarily dependent upon the energy of the injected electron/hole and the carrier diffusion coefficient of the sample specimen. Typical STM electron energies are in the 0-5 eV range, quite low compared to other luminescence microscopies², limiting the extent of carrier diffusion and thus also localizing light emission to a small region directly beneath the STM tip.^{2,3}

3. Drift limitations of the STM: Due to the low quantum efficiencies of most tunneling luminescence processes, long acquisition times are required to achieve a satisfactory signal to noise (SNR) ratios.² For stable scanning/luminescence measurements, this requires a STM with low thermal drift properties. As a further means for reducing thermally induced lateral drift, some researchers opt to perform STL measurements at ultra-low temperatures (<80K).⁴

Lateral resolution for STL measurements customarily reaches the nanometer range and thus presents exciting new opportunities for the optical characterization of materials and structures. “For example, when one applies [STL] to the study of quantum nanostructures, one can identify an individual structure by STM imaging, and then obtain the optical spectra from that specific structure. Thus, one can directly gain information on the size and shape dependence of the electronic transitions (quantum confinement effect).²” In addition to high spatial resolution, STL also is relatively non-invasive and non-perturbative to the structures probed, with *tunneling* electrons as the exciting particles, no actual physical contact with the sample surface is necessary. Additionally, no complicated light sources are required to probe the optical structure of the specimen

Despite the considerable advantages of high-resolution and non-invasiveness, STL does have a number of drawbacks, making it unsuitable for use on some material systems. In order for electrons to tunnel effectively, the sample specimen must be either conducting or semiconducting. The STL

technique can thus not be used to probe structures that exhibit insulating electronic character. In addition, for optimal tunneling stability, STL measurements should be carried out within an ultrahigh vacuum (UHV) environment, requiring that all specimens be UHV-compatible. As a result, STL generally cannot be performed on living or hydrated samples such as cells or proteins. And finally, as STM/STL are surface-sensitive techniques, any structures probed must be supported on a solid substrate, precluding the analysis of any solution-based structures by this approach.

STL METHODS AND INSTRUMENTATION

Sakurai, et. al. identify four fundamental light emission mechanisms in STL depending upon the nature of the specimen probed.⁵ These four luminescence processes are outlined below and shown schematically in Figure 2.⁵

1. Tip-induced excitation of surface plasmons in metallic surfaces: Tunneling electrons injected into noble-metal surfaces excite localized surface plasmons which subsequently may emit light upon relaxation. Photons emitted by this process have a frequency approximately equal to the localized surface plasmon resonance frequency and are emitted with a quantum efficiency of $\sim 10^{-4}$ photons/injected electron.

2. Electron-hole recombination in direct gap semiconducting surfaces: Minority carriers injected into doped semiconducting samples recombine with readily available majority carriers across the electronic bandgap, emitting light of energy equal to the bandgap energy $E_g = h\nu$, with a quantum efficiency of $\sim 10^{-4}$ photons/injected carrier. One should note that light emission will occur only when *minority*

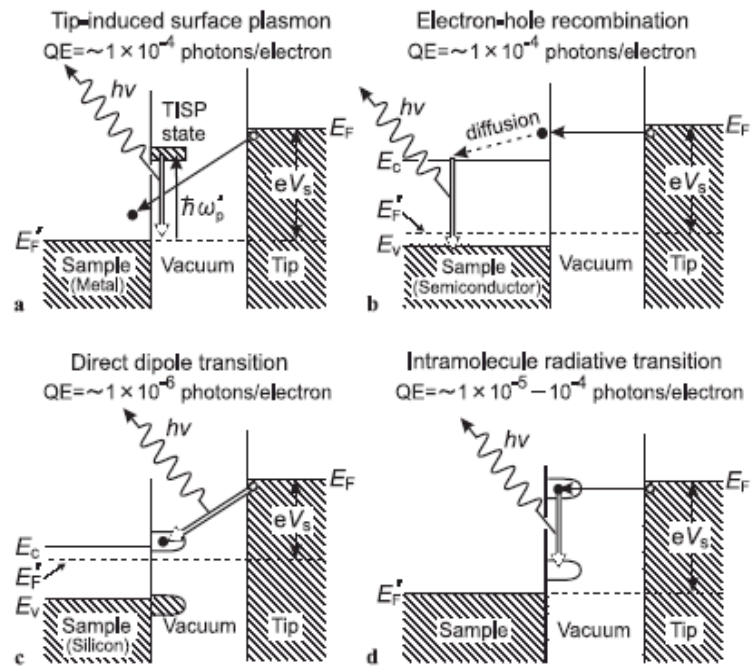


Figure 2: Schematic illustration of the four tunneling luminescence processes possible in STL. Figure from reference 5.

carriers are injected into doped semiconducting sample: holes must be injected into a p-type sample and electrons injected into an n-type sample in order for STL studies to be carried out.² For the case of injected majority carriers, the minimal number of minority carriers available for recombination prevents the generation of a useful photon flux.

3. Direct dipole transitions in general materials: In certain materials, direct radiative transitions between the surface states of the tip and sample can occur during the electron tunneling process. Such direct dipole transitions occur relatively infrequently, with a quantum efficiency of $\sim 10^{-6}$ photons/ injected electron.

4. Intramolecular radiative transitions in organic molecules: For organic molecules tethered to a surface, tunneling carriers from the tip can be injected directly into high-lying molecular orbitals. Light emission occurs as the electron transitions to a lower energy state within the molecule, generating a photon of energy equal to the molecular level spacing with a quantum efficiency of $\sim 10^{-4}$ - 10^{-5} photons/injected electron.

In order to induce and detect tunneling luminescence through the processes above, all experiments must be carried out with the utmost care in a precision STL system. As Ushioda outlines, effective STL instrumentation must include the following components:² a stable STM and its associated control electronics, a light collection/transmission apparatus, some sort of wavelength selection device, a photon detector/counter, and a personal computer or other device for data storage and analysis. The above components are examined below in further detail.

As STL is essentially a luminescent extension of scanning tunneling microscopy, the availability of a stable, low drift STM is critical to the successful implementation of any tunneling luminescence scheme. In order to achieve sub-nanometer spatial resolution in imaging and spectroscopy, the STM and its control electronics must possess excellent vibration isolation, extremely low electronic noise (tunneling currents tend to be on the order of 1 nA), and the ability to realize lateral and vertical positioning with sub-angstrom precision. In addition, due to the long photon collection times necessary to obtain a satisfactory SNR in STL (Ushioda cites collection times of hundreds of seconds per spectrum²), the STM must also exhibit extremely low lateral drift properties to ensure the fidelity of the detected light signal.

Aside from the STM scanner itself, the light collection instrumentation is the most complicated and varied segment of the STL set-up. A survey of the literature suggests that there are three primary approaches that have been implemented in order to collect light emitted from the tunnel junction and

transmit it to an external photodetector: 1. far field detection schemes making use of both *in* and *ex situ* lenses and/or mirrors, 2. optical fiber collection and transmission methods, and 3. conductive transparent STM tip collectors.

In common far field detection schemes,^{2,6} a lens is placed within the STM UHV chamber, “near” to the tip/sample tunnel junction (though geometric concerns generally prevent the lens from coming closer than

several centimeters from the junction) and directs collected photons out of the system through a viewport mounted on the chamber wall (Figure 3). Directly outside of the viewport, a second lens and/or fiber optic cable directs transmitted light to the photon detector and analyzer. While generally effective at capturing emitted light, the solid angle of collection in these lens-based systems can be rather small (~0.2-1 steradians^{7,8}) necessitating longer collection times. To enhance total light collection, parabolic mirrors can be appropriately placed within the UHV chamber to collect and collimate emitted photons, dramatically increasing the intensity of the detected luminescence signal.^{4,8} While many groups find such far field detection schemes adequate, they can be somewhat bulky, and the necessity of optical access to the tunnel junction through a chamber viewport makes them sometimes inconvenient for use with low temperature STM systems in which the radiation leaks from chamber windows are extremely undesirable.

A second light collection implementation makes use of optical fibers to collect photons emitted from the tunnel junction and transmit them to an external photodetector.^{2,9,10} As shown in Figure 4, light collection is achieved by placing the end of silica optical fibers “close” to the tip/sample junction, where “close” can be quantified in the following manner. Approximating the sample emitter as a point source, it can be shown that the maximum solid angle of photon collection for a single optical fiber is attained when⁹

$$D \leq D_0 = \frac{d/2}{\tan(\sin^{-1}(NA))}$$

with D the distance between the sample junction and the fiber end, d the diameter of the fiber core, and NA the numerical aperture of the optical fiber which is dependent on the fiber core/cladding material combination. As long as the distance between the optical fiber end and the tunnel junction is less than the critical distance, D_0 , the maximum solid angle of collection can be achieved with proper fiber alignment. Arafune, et. al., note, though, that for a single silica optical fiber of diameter, $d=600\mu\text{m}$ and $NA=0.2$, the total solid angle of collection achievable of 0.13 steradians is comparable to that achievable with a

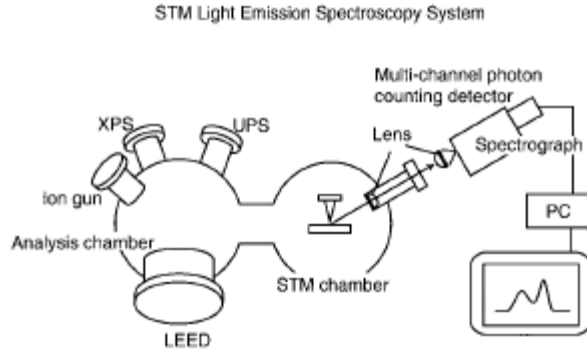


Figure 3: Typical lens set-up for STL measurements in UHV. Figure from reference 2.

standard lens system.⁹ As a result, these scientists opted to place multiple fibers within the vicinity of the junction to increase the total collected solid angle, and, with four optical fibers positioned appropriately, they were able to increase the solid angle of their collection apparatus by a factor of 2.6 over that achieved using a single silica fiber.⁹

In the conductive transparent (CT) tip approach pioneered by Murashita and coworkers at NTT in the 1990's,^{3,11} the STM tip itself acts as both the injector of tunneling electrons as well as the collector of emitted photons. Such a scheme circumvents the need for a bulky external collection source, as emitted light is collected by the proximal tip and directed towards a detector through an attached optical transmission fiber. The CT tip itself is composed of GeO₂ doped silica fiber, a material chosen for its minimal outgassing properties in UHV. A multimode fiber with 100 μm core diameter was found to provide sufficient collection and transmission capabilities. The tip backend was ground flat and plated with antireflective coating to enhance the optical coupling between the tip and a second transmission fiber, while the front end was tapered through a dual-step mechanical and electrochemical-etching process to an end apex radius of ~100 nm. To provide the metallicity necessary of any STM tip, an ~70 nm layer of the transparent conductive oxide, In₂O₃, was deposited onto the tip end, with a subsequent ~40 nm ultrathin Au layer introduced to stabilize the metal apex during scanning(Figure 5).¹¹

Murashita suggests that in addition to eliminating unwieldy external collection sources, the CT STL method improves upon standard lens detection schemes in two further ways:¹¹ Due to the nanoscale dimensions of the tip apex, the CT will only be sensitive to light emitted from a small region localized directly beneath the tip end, with photons emitted from more remote regions of the sample (which are collected by the lens in farfield detection schemes) excluded from the CT collected light, providing an improvement in STL spatial resolution. Additionally, an enhancement in collection yield is attained due to the position of the collecting tip normal

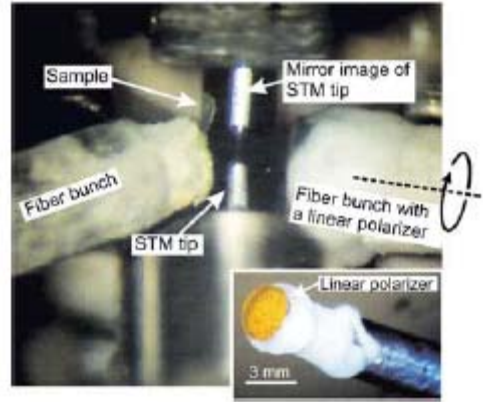


Figure 4: Photograph of a fiber optic collector in the vicinity of the tip/sample tunnel junction. This set-up also has a second fiber bunch for polarized luminescence measurements. From reference 5.

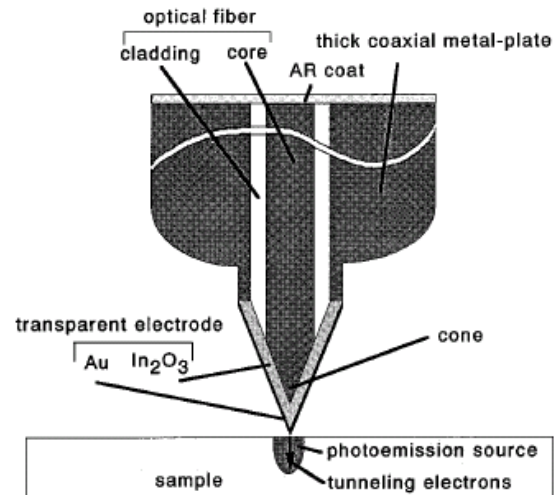


Figure 5: Schematic diagram of Murashita's CT STL photon collection implementation. Figure from reference 11.

to the emitting surface. With the CT tip directly over the active surface region, photons emitted orthogonally from the sample, which represent a majority of emitted photons for many samples,¹¹ are easily collected, while in other collection schemes, such photons are blocked from detection by the presence of a non-collecting metallic tip. In fact, Murashita estimates a 100-fold increase in collected intensity using the CT tip over traditional lens collection schemes.³

However, the introduction of a conductive-transparent tip into a UHV system is far from trivial, and, judging from the literature, in spite of these advantages it appears that the CT tip STL implementation is rarely used in actual practice.

Photon detection and analysis is generally achieved through the use of a grating monochromator^{4,9,11} for wavelength discrimination in series with a charged coupled device (CCD) camera^{3,4,9-11} or optical multichannel analyzer (OMA)^{6,10} for photon detection/counting. Generally, the recorded wavelength and intensity data is digitized and stored locally on a personal computer for later retrieval and analysis. Photon maps and spectra can then be generated and analyzed according to the experimenter's aims.

STL OF MOLECULES AND NANOSTRUCTURES

The high spatial resolution possible with STL and its relative non-invasive nature make it an ideal technique for studying the optical characteristics of surface-tethered molecules and other nanostructures. STL experiments involving two relevant classes of optically active nanostructures, organic molecules and quantum dots, will be highlighted in the following paragraphs.

STL of Organic Molecules on Surfaces

One of the most elegant illustrations of STL's utility in probing single molecules was reported in *Science Magazine* in 2003.¹² Members of Wilson Ho's group used low temperature scanning tunneling microscopy and luminescence to detect optical transitions within Zn(II)-etioporphyrin I (ZnEtiol) molecules deposited onto an Al₂O₃ coated NiAl(110) surface, demonstrating the sensitivity of light emission to a molecule's geometric conformation and providing perhaps the most compelling evidence of tunneling-electron induced intramolecular radiative transitions to date. In their study, Ho and coworkers used traditional STM to identify six different conformations the ZnEtiol molecule can take upon adsorption onto the Al₂O₃/NiAl surface. Through luminescence spectroscopy, it was found that only two of the six molecular conformations emitted light. Spectra acquired from these two emitters are shown in Figure 6, and, based on these measurements, the authors reported several other notable observations. The

lower panels of Figure 6 depict TL spectra acquired from each molecule at varying sample bias. It can be seen that the peak energies are invariant under changing sample bias- indicating that the observed light emission arises from a tip-independent process, and Ho, et. al. convincingly argue that these photons are emitted during radiative intramolecular transitions. Additionally, the authors note that light emission arising from the two different conformations exhibit distinctly different spectral features, confirming the dependence of these radiative transitions on the geometric configuration of the ZnEtiol molecule. Furthermore, as shown in the central panels of Figure 6, different regions *within* a single ZnEtiol exhibit significant differences in emission intensities, which they attribute to the spatial non-uniformity of higher energy molecular states.

The efforts of Ho, et. al. marked an important step in the development of single-molecule spectroscopy and fluoroscopy techniques. Their STL instrumentation provided a spatial resolution of ~ 8 nm, allowing them to track radiative differences within the ZnEtiol molecule itself. The non-perturbative nature of the STL technique prevented molecular desorption or other significant molecular disturbance during experimentation. Additionally, the use of a thin insulating Al_2O_3 layer proved a critical component of the structure, preventing quenching of ZnEtiol photon emission which can arise from the molecule's interactions with the metallic NiAl(110) substrate.

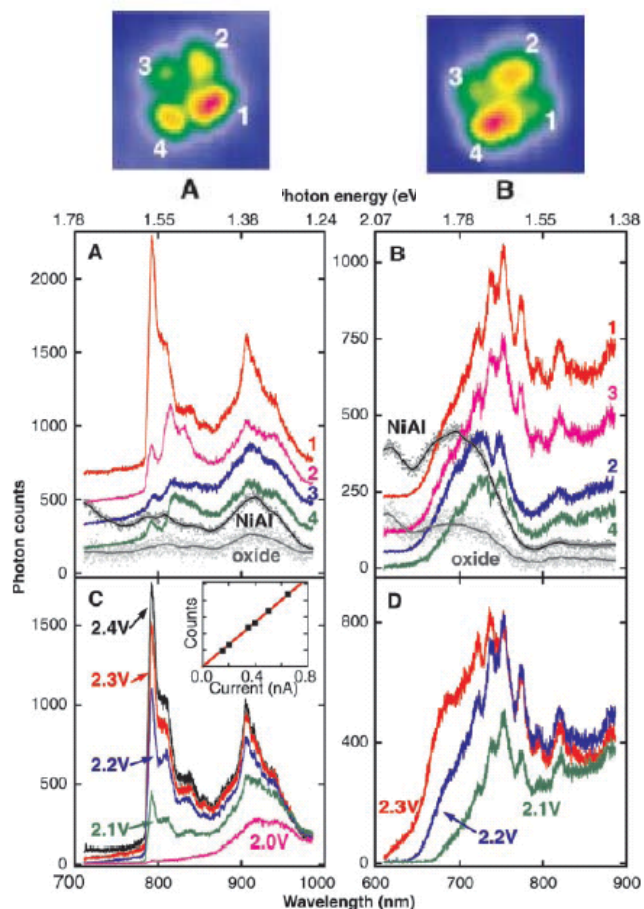


Figure 6: Composite image from reference 12- Upper Panels: STM dI/dV spatial mappings of two conformations, A and B, of the ZnEtiol molecule observed on the $\text{Al}_2\text{O}_3/\text{NaCl}$ substrate. Central Panels, A-B: spectra acquired at various positions on the A and B configured molecules, respectively. Spectra labeled 1-4 acquired at correspondingly labeled lobes on the above STM spatial mappings. Lower Panels, C-D: Emission spectra acquired from molecules A and B, respectively, at varying sample bias. For further image details, refer to reference 12.

STL of Semiconducting Quantum Dots

Among the structures that may benefit most from STL studies are III/V-semiconductor based embedded quantum dots (QDs). The optical properties of individual QDs are extremely difficult to discern, as the most common optical characterization techniques, like photoluminescence, sample an ensemble of dots, leading to a broadening in the observed spectra relative to individual dot emission. However, by using STL, several groups have reported the observation of tunneling-induced emission from individual QDs.^{13,14} Among these, Yamanaka and coworkers were able to identify individual emitting dots through spatially resolved photon maps and obtain associated emission spectra of these discrete structures.¹⁴ In their work, undoped InAs QDs with diameters ~ 20 nm grown by the Stranski-Krastanov approach, were formed on an n-type GaAs substrate and capped with an ~ 20 nm n-type GaAs buffer layer. The lateral density of dots was kept to $\sim 5.5 \times 10^{10} \text{ cm}^{-2}$ to provide a spatial separation between distinct QDs sufficient for individual dot identification via low temperature (120 K) STM. The total intensity photon map shown in Figure 7(a) depicts the luminescence from a single InAs dot just beneath the scanning surface. The luminescent region possesses a diameter of ~ 50 nm, approximately twice the suspected size of the 20 nm diameter InAs dots, a broadening the authors attribute to lateral carrier diffusion within the GaAs cap layer.¹⁴ Additionally, the current-voltage tunneling parameters (1 μA tunneling current, -10 V sample bias) used to acquire the STL image were rather high compared to typical STM setpoints, presumably to ensure carrier injection through the cap layer into the buried dots, and may have also contributed to the observed spatial broadening. The spectra of the luminescent region plotted in Figure 7(b) shows a clear, narrow peak at ~ 980 nm, corresponding to the light emission from a single InAs QD. The authors note that the peak linewidth is limited by their instrumentation and does not exhibit the broadening characteristic of ensemble measurements, confirming their assignment of the spectral feature to an individual dot.

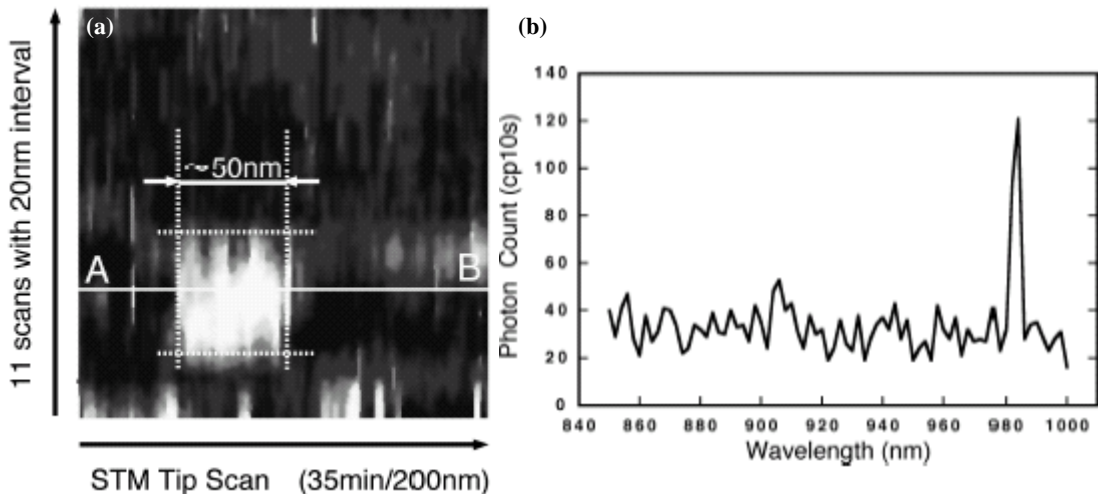


Figure 7: (a) STL total intensity photon map. Bright portion corresponds to emission from individual InAs QD. (b) Emission spectra luminescent region of sample. Narrow peak at ~ 980 nm corresponds to light emission from a single InAs QD. Images from reference 14.

PROPOSAL: STL OF SINGLE-WALLED CARBON NANOTUBES

My personal thesis research involves using scanning tunneling microscopy to probe the electrical and physical (but *not* optical) properties of single-walled carbon nanotubes (SWNTs). These nearly one-dimensional molecules, which are essentially sheets of graphene rolled into a tubular structure, have tube diameters on the order of a nanometer and lengths that can reach several microns or more, and have garnered much interest in the past decade for their potential utility in a variety of electronic, chemical, and mechanical nanodevices.¹⁵ The fluorescence properties of SWNTs in solution have been studied extensively,^{16,17} though such measurements are inherently ensemble averages. While there have been a number of reports of individual nanotube luminescence measurements,¹⁸⁻²⁰ in learning about STL, I believe this technique could offer a unique opportunity for probing the optical characteristics of distinct carbon nanotubes with incredible spatial resolution. I know from personal experience that SWNTs are UHV-compatible and can easily be applied to metallic or semiconducting surfaces for analysis with STM. Electrically induced optical emission from SWNTs has been observed,²¹ suggesting that tunneling-electron induced luminescence should be possible. Also- there have been several reports of tunneling-induced luminescence on C-60,^{22,23} a close molecular relative of carbon nanotubes, again indicating the feasibility of performing STL on these structures. My literature search turned up little in the way of STL attempts on carbon nanotubes. The sole item I found was a report in which Cortager, et. al. performed limited STL measurements on bundles of multi-walled carbon nanotubes.²⁴ However, it appears that there has been no published work on the tunneling-electron induced light emission from individual SWNTs. Perhaps this dearth of publications indicates that there are other significant barriers to STL on SWNTs of which I am not aware. However, if one were able to detect TL on these structures with nanometer-scale resolution, a whole host of interesting questions could potentially be answered or explored: Does luminescence occur uniformly along the length of the tube? Do the presence of the nanotube endcaps, kinks, or defects modify the tube's optical emission properties? How is a nanotube's emission altered by the surface on which it is supported and its proximity to other nanotubes? Can its optical emission properties be correlated with its electronic structure? And there is much more that could be learned, I am sure. Overall, though it may be difficult and present an array of challenges and obstacles that would need to be overcome, I think the application of STL to single-walled carbon nanotubes could be a worthwhile venture.

REFERENCES

- ¹J.K. Gimzewski, B. Reihl, J.H. Coombs, and R.R. Schlittler, "Photon emission with the scanning tunneling microscope," *Zeitschrift fur Physik B* **72** (1988) 497-501.
- ²S. Ushioda "Probing individual nanostructures with STM-induced light emission," *Solid State Communications* **117** (2001) 159-166.
- ³T. Murashita, "Optical system for tunneling-electron luminescence spectro/microscopes with conductive-transparent tips in ultrahigh vacuums," *J. Vac. Sci. Technol. B* **17**(1) Jan/Feb (1999) 22-28.
- ⁴Y. Khang, Y. Park, M. Salemeron, and E.R. Weber, "Low temperature ultrahigh vacuum cross-sectional scanning tunneling microscope for luminescence measurements," *Rev. Sci. Inst.* **70** (1999) 4595-4599.
- ⁵M. Sakurai, C. Thirstrup, and M. Aono, "New aspects of light emission from STM," *Applied Physics A* **80** (2005) 1153-1160.
- ⁶S. Alvarado, W. Reiss, P. Seidler, and P. Strohriegl, "STM-induced luminescence study of poly(p-phenylenevinylene) by conversion under ultraclean conditions," *Phys. Rev. B* **56** (1997) 1269-1278.
- ⁷D. Abraham, A. Veider, Ch. Schonenberger, H. Meier, D. Arent, and S. Alvarado, "Nanometer resolution in luminescence microscopy of III-V heterostructures," *Appl. Phys. Lett.* **56** (1990) 1564-1566.
- ⁸R. Berndt, R. Schlittler, and J. Gimzewski, "Photon emission scanning tunneling microscope," *J. Vac. Sci. Technol. B* **9** (1991) 573-577.
- ⁹R. Arafune, K. Sakamoto, K. Meguro, M. Satoh, A. Arai, and S. Ushioda, "Multiple-Fiber Collection System for Scanning Tunneling Light Emission Spectroscopy," *Jpn. J. Appl. Phys.* **40** (2001) 5450-5453.
- ¹⁰R. Pechou, R. Cortager, F. Ajustron, and J. Beauvillain, "Control of light emission from an STM and surface modifications," *Surface Science* **418** (1999) 1-7.
- ¹¹T. Murashita, "Novel conductive transparent tip for low-temperature tunneling-electron luminescence microscopy using tip collection," *J. Vac. Sci. Technol. B* **15** (1997) 32-37.
- ¹²X. Qiu, G. Nazin, and W. Ho, "Vibrationally resolved fluorescence excited with submolecular precision," *Science* **299** (2003) 542-546.
- ¹³U. Hakanson, M. Johansson, M. Holm, C. Pryor, L. Samuelson, W. Seifert, and M. Pistol, "Photon mapping of quantum dots using a scanning tunneling microscope," *Appl. Phys. Lett.* **81** (2002) 4443-4445.

- ¹⁴K. Yamanaka, K. Suzuki, S. Ishida, and Y. Arakawa, "Light emission from individual self-assembled InAs/GaAs quantum dots excited by tunneling current injection," *Appl. Phys. Lett.* **73** (1998) 1460-1462.
- ¹⁵V.N. Popov, "Carbon nanotubes: properties and application," *Mat. Sci. and Eng. R* **43** (2004) 61-102.
- ¹⁶M.J. O'Connell, S.M. Bachilo, C.B. Huffman, V.C. Moore, M.S. Strano, E.H. Haroz, K.L. Rialon, P.J. Boul, W.H. Noon, C. Kittrell, J. Ma, R.H. Hauge, R.B. Weisman, and R.E. Smalley, "Band Gap Fluorescence from Individual Single-Walled Carbon Nanotubes," *Science* **297** (2002) 593-596.
- ¹⁷S.M. Bachilo, M.S. Strano, C. Kittrell, R.H. Hauge, R.E. Smalley, and R.B. Weisman, "Structure-Assigned Optical Spectra of Single-Walled Carbon Nanotubes," *Science* **298** (2002) 2361-2366.
- ¹⁸A. Hagan, M. Steiner, M.B. Raschke, C. Lienau, T. Hertel, H. Qian, A. Meixner, and A. Hartschuh, "Exponential Decay Lifetimes of Excitons in Individual Single-Walled Carbon Nanotubes," *Phys. Rev. Lett.* **95** (2005) 197401.
- ¹⁹J. Lefebvre, J.M. Fraser, P. Finnie, and Y. Homma, "Photoluminescence from an individual single-walled carbon nanotube," *Phys. Rev. B* **69** (2004) 075403.
- ²⁰D.A. Tsyboulski, S.M. Bachilo, and R.B. Weisman, "Versatile Visualization of Individual Single-Walled Carbon Nanotubes with Near-Infrared Fluorescence Microscopy," *NanoLetters* **5** (2005) 975-979.
- ²¹J.A. Misewich, R. Martel, Ph. Avouris, J.C. Tsang, S. Heinze, and J. Tersoff, "Electrically Induced Optical Emission from a Carbon Nanotube FET," *Science* **300** (2003) 783-786.
- ²²R. Berndt, R. Gaisch, J.K. Gimzewski, B. Reihl, R.R. Schlittler, W.D. Schneider, M. Tschudy, "Photon Emission at Molecular Resolution Induced by a Scanning Tunneling Microscope," *Science* **262** (1993) 1425-1427.
- ²³E. Cavar, M.-C. Blum, M. Pivetta, F. Patthey, M. Cherqui, and W.-D. Schneider, "Fluorescence and Phosphorescence from Individual C₆₀ Molecules Excited by Local Electron Tunneling," *Phys. Rev. Lett.* **95** (2005) 196102.
- ²⁴R. Coratger, J.-P. Salvetat, A. Carlados, F. Ajustron, J. Beauvillain, J.-M. Bonard, and L. Forro, "STM induced luminescence in carbon nanotubes," *Eur. Phys. J. AP* **15** (2001) 177-180.